Pressure-induced spin fluctuations and spin reorientation in hexagonal manganites

2007 J. Phys.: Condens. Matter 19 156228

(http://iopscience.iop.org/0953-8984/19/15/156228)

IOP PUBLISHING JOURNAL OF PHYSICS: CONDENSED MATTER

J. Phys.: Condens. Matter **19** (2007) 156228 (9pp) doi:10.1088/0953-8984/19/15/156228

Pressure-induced spin fluctuations and spin reorientation in hexagonal manganites

D P Kozlenko[1], S E Kichanov[1], S Lee[2], J-G Park[2,3] and B N Savenko[1]

[1] Frank Laboratory of Neutron Physics, Joint Institute for Nuclear Research, 141980 Dubna, Russia
[2] Department of Physics and Institute of Basic Science, SungKyunKwan University, Suwon 440-746, Korea
[3] Center for Strongly Correlated Materials Research, Seoul National University, Seoul 151-742, Korea

Received 18 January 2007, in final form 21 February 2007
Published 27 March 2007
Online at stacks.iop.org/JPhysCM/19/156228

Abstract

The magnetic structures of hexagonal manganites $YMnO_3$ and $LuMnO_3$ have been studied by powder neutron diffraction up to 6 GPa in the temperature range 10–295 K. At ambient pressure, a triangular antiferromagnetic (AFM) state of a Γ_1 irreducible representation is stable below $T_N = 70$ K in $YMnO_3$. Upon the application of high pressure, a spin reorientation is induced and the triangular AFM structure evolves from Γ_1 to $\Gamma_1 + \Gamma_2$ representations. On the other hand, in $LuMnO_3$ the triangular AFM state of a Γ_2 irreducible representation with $T_N \approx 90$ K remains stable over the entire pressure range investigated. The ordered magnetic moment values decrease under pressure with $dM/dP = -0.35\ \mu_B\ GPa^{-1}$ in $YMnO_3$ and $-0.08\ \mu_B\ GPa^{-1}$ in $LuMnO_3$. Simultaneously, a considerable increase in diffuse scattering intensity was found in $YMnO_3$, while it was much less pronounced for $LuMnO_3$. Both features indicate the enhancement of spin fluctuations due to geometrical frustration effects and an increase in the volume fraction of the spin-liquid state coexisting with the ordered AFM phase. The characteristic spin correlation length is weakly affected by pressure. The relationship between the pressure-induced behaviour of magnetic structure and the structural characteristics of the quasi-two-dimensional (2D) triangular network formed by Mn and O ions in hexagonal $RMnO_3$ is analysed.

1. Introduction

Manganites $RMnO_3$ exhibit a rich variety of physical properties depending on the rare-earth (R) element type. Compounds with the larger ionic radius of R-elements (La, Pr, Nd, Sm, Eu, Gd, and Tb) crystallize in the orthorhombic structure of $Pnma$ symmetry [1]. In compounds with smaller ionic radius (Ho, Er, Tm, Yb, Lu, Y, Sc and In) a hexagonal structure of $P6_3cm$

symmetry is stabilized [2]. Hexagonal manganites belong to an unusual class of multiferroic materials showing the coexistence of ferroelectric behaviour and magnetic ordering. The ferroelectric transition temperature is found to be much higher, $T_C \sim$ 600–900 K, than the antiferromagnetic (AFM) ordering temperature, $T_N \sim$ 70–130 K [3]. However, we note that magnetic Curie–Weiss temperatures are around 500–700 K in most of hexagonal manganites, which indicates that somehow the magnetic ordering is significantly suppressed.

In the hexagonal structure of $RMnO_3$, Mn ions are located at the centres of MnO_5 bipyramids and they form a natural 2D corner-sharing triangular network separated along the *c*-axis by a non-coplanar layer of R atoms, which leads naturally to geometrically frustrated magnetism. The distance between the nearest Mn atoms is ∼3.5 Å in the *ab* plane and ∼6 Å along the *c*-axis, respectively. Thus a dominant magnetic interaction is the in-plane Mn–O–Mn antiferromagnetic superexchange, while the Mn–O–O–Mn superexchange between adjacent triangular planes is about two orders of magnitude weaker [4, 5].

Magnetic properties of $RMnO_3$ manganites depend strongly on the ionic radius of the R cation (r). For example, $InMnO_3$ with the largest r value does not exhibit long-range magnetic order at temperatures down to 5 K [6]. On the other hand, $YMnO_3$ exhibits a triangular AFM structure of Γ_1 (or Γ_3) irreducible representation symmetry below $T_N = 70$ K [4, 7–9]. Systems with smaller r values, e.g. $HoMnO_3$, $ErMnO_3$, $TmMnO_3$, $YbMnO_3$, $LuMnO_3$ and $ScMnO_3$, exhibit AFM orderings below around 100 K, which can be described by Γ_2 (or Γ_4) irreducible representations [7, 10–15]. These four magnetic structures (Γ_1, Γ_2, Γ_3 and Γ_4) have different types of magnetic coupling between adjacent triangular Mn planes: AFM coupling for Γ_1 (Γ_2) and FM coupling for Γ_3 (Γ_4) representations. In addition, spin-reorientation phase transitions were observed at $T_R < T_N$ for $ScMnO_3$ and $HoMnO_3$ [7, 10–14].

The observed rich variety of the magnetic properties of hexagonal manganites reflects a delicate balance between magnetic interactions, which can be easily modified by changes of the geometry of the Mn–O–Mn network depending on the r value. Apart from the variation of the ionic radius of the R cation, interatomic distances and angles in the structure can also be modified directly by the application of high external pressure. Recent structural studies revealed a suppression of the ordered Mn magnetic moment in $YMnO_3$ at high pressures, presumably due to an enhancement of spin fluctuations [16, 17]. A possibility of the spin reorientation at $P \sim 2.5$ GPa in $YMnO_3$ was also suggested [16]. However, the pressure behaviour of the ordered magnetic moment and spin-reorientation angle remains not well established. In the work in [17], only a restricted pressure range up to 0.8 GPa was investigated. In the study in [16], the magnetic structure of $YMnO_3$ was analysed only at the two pressure points of 2.5 and 5 GPa and, due to the rapid suppression of magnetic peak intensity and the low statistics of diffraction data, only rough estimations of the ordered magnetic moment values and spin-reorientation angle were obtained.

In order to study in detail the pressure-induced modifications of the magnetic state of $YMnO_3$ and hexagonal manganites in general and to clarify the relationship with the behaviour of the crystal structure, we have performed neutron diffraction experiments at high external pressures of up to 6 GPa with $YMnO_3$ and $LuMnO_3$ compounds. These compounds have different AFM ground states at ambient pressure and no magnetic moment at the R sublattice.

2. Experimental details

Polycrystalline $YMnO_3$ and $LuMnO_3$ samples were synthesized by using the standard solid-state reaction method. Cation oxides of Y_2O_3 or Lu_2O_3 (99.999%) and Mn_2O_3 (99.999%) were thoroughly mixed in order to achieve a homogeneous mixture. The mixed powders were then heated to, and kept at, 900 °C for 12 h before subsequent annealing at 1100 °C for 24 h and

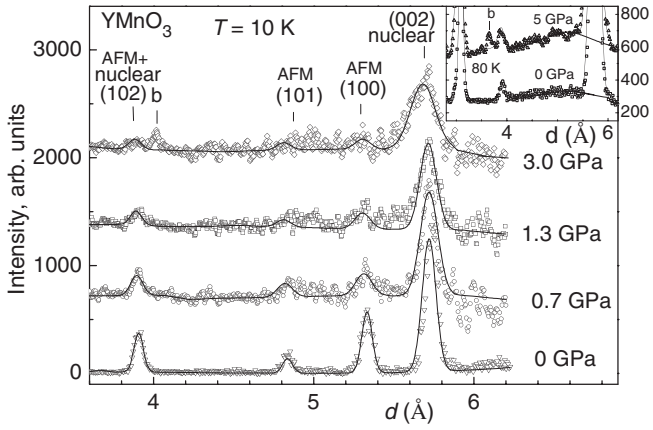

Figure 1. Parts of neutron diffraction patterns of $YMnO_3$ measured at selected pressures for $T = 10$ K (GEM data, $2\theta = 34.96°$) and 80 K (inset, DN-12 data, $2\theta = 45.5°$). The data points are marked by symbols and the lines represent our Rietveld refinement results. The diffuse scattering peak at $d \approx 5.1$ Å for 80 K data was fitted by a Lorentzian. The indexes of the peaks with a magnetic contribution are given. The weak peak marked by 'b' corresponds to a Bragg peak coming from the pressure cell.

at 1200 °C for 24 h with intermediate grindings. A final sintering was performed at 1350 °C for 24 h. The purpose of the intermediate grindings was to prevent the formation of impurity phases. The x-ray diffraction measurements at room temperature showed that the samples form in a single phase of the hexagonal $P6_3cm$ structure.

Neutron powder diffraction measurements at ambient pressure and high external pressures of up to 6 GPa were performed at selected temperatures in the range 10–290 K with the GEM diffractometer (ISIS pulsed neutron source Rutherford Appleton Laboratory, UK) and also the DN-12 spectrometer (IBR-2 high-flux pulsed reactor, Frank Laboratory of Neutron Physics, Joint Institute for Nuclear Research, Russia) using sapphire anvil high pressure cells [18] with a sample volume of about 2 mm^3. Several tiny ruby chips were placed at different points of the sample surface to monitor the pressure distribution. The pressure was determined using the ruby fluorescence technique with an accuracy of 0.05 GPa at each ruby chip, and the pressure value on the sample was determined by averaging the pressure values read off from the ruby chips. The estimated inhomogeneity in the pressure distribution on the sample surface was less than 20%. Diffraction patterns were collected by detector banks located at scattering angles of 34.96° (GEM), 45.5° and 90° (DN-12) with resolutions of $\Delta d/d \approx 0.017$ (GEM), 0.022 and 0.015 (DN-12) for these angles, respectively. Typical data collection time at each temperature were 20 h (DN-12) and 12 h (GEM). Experimental data were analysed by the Rietveld method using the MRIA program [19] or Fullprof [20] when magnetic structure was to be included.

3. Results and discussion

Neutron diffraction patterns of $YMnO_3$ and $LuMnO_3$ measured at selected pressures and temperatures are shown in figures 1 and 2. Over the whole pressure (0–6 GPa) and temperature (10–300 K) ranges studied, the hexagonal crystal structure of $P6_3cm$ symmetry remains unchanged. In $YMnO_3$, there appear magnetic peaks (100) at $d = 5.31$ Å and (101) at $d = 4.82$ Å (this peak is not purely magnetic, but the nuclear contribution is almost negligible) and a magnetic contribution to the nuclear peak (102) at $d = 3.88$ Å at ambient pressure on

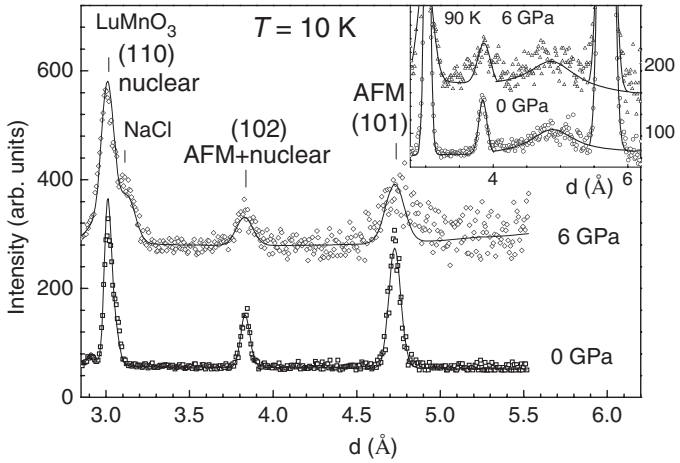

Figure 2. Parts of neutron diffraction patterns of $LuMnO_3$ measured at selected pressures for $T = 10$ K ($2\theta = 90°$) and 90 K (inset, $2\theta = 45.5°$) at the DN-12 spectrometer. The data points are marked by symbols and the lines represent our Rietveld refinement results. The diffuse scattering peak at $d \approx 4.9$ Å for 90 K data was fitted by a Lorentzian. The indexes of the peaks with a magnetic contribution are given. NaCl was added to the sample to reduce pressure gradients.

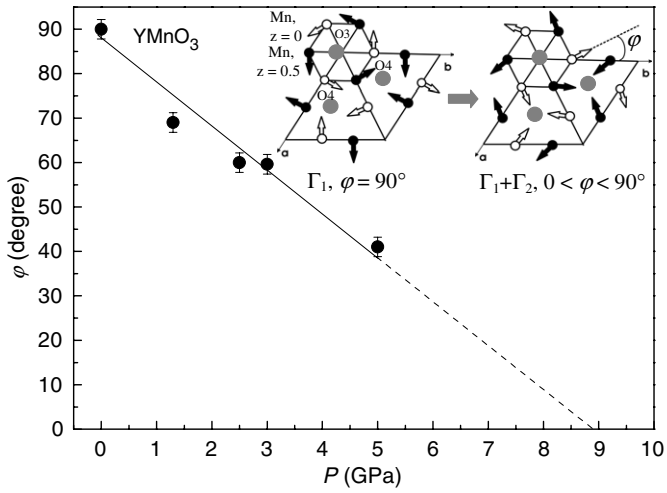

Figure 3. The angle φ between the Mn magnetic moments (at 10 K) and hexagonal axes in $YMnO_3$ fitted by a linear function (solid line) and its extrapolation up to 9 GPa (dashed line). The relevant modification of the magnetic structure symmetry from initial Γ_1 towards $\Gamma_1 + \Gamma_2$ is also illustrated.

cooling below $T_N = 70$ K, indicating an onset of the triangular 120° AFM state. Refinements of the magnetic structure with Γ_1 and Γ_3 irreducible representations models have given nearly the same fitting quality and magnetic moments values. However, in a previous neutron diffraction study [7] with a higher resolution, it was demonstrated that the Γ_1 representation model is in better agreement with the experimental data at ambient pressure than was the Γ_3 representation model. Finally, the Γ_1 representation model (figure 3) of the magnetic structure with Mn magnetic moments lying in the *ab* plane was chosen for the analysis of our high-pressure data. The value of the ordered Mn magnetic moment is determined to be 3.27(5) μ_B at $T = 10$ K

Table 1. Ordered magnetic moments and angle between their directions and hexagonal axes in the *ab* plane for $YMnO_3$ and $LuMnO_3$ at selected pressures and $T = 10$ K.

	$YMnO_3$			$LuMnO_3$		
P (GPa)	0	3	5	0	3	6
μ (μ_B)	3.27(5)	2.12(7)	1.52(9)	2.48(5)	2.28(7)	1.98(9)
φ (deg)	90	59.6(7)	41.0(9)	0	0	0
R_p (%)	7.11	11.3	10.5(9)	5.70	5.98	8.67
R_{wp} (%)	8.32	11.9	11.1	5.74	6.07	9.33

(table 1), which is in good agreement with previous studies of $YMnO_3$ at ambient pressure [7–9] and considerably smaller than the expected value of 4.0 μ_B for Mn^{3+}.

Above the magnetic ordering temperature we observed a noticeable diffuse scattering in the d-spacing range of 4 Å $< d <$ 6 Å (figure 1). This feature as well as the reduced value of the ordered Mn magnetic moment, we believe, result from geometrical frustration effects due to the triangular arrangement of Mn ions. The strong diffuse scattering in $YMnO_3$ was attributed to the formation of a spin-liquid state which coexists with the magnetically ordered AFM phase well below T_N [9].

$YMnO_3$ displays a substantial decrease and relative change in the intensities of magnetic peaks under high pressure at $T < T_N \approx 70$ K (figure 1). As we increase pressure, the intensity ratio of the $I_{(100)}/I_{(101)}$ magnetic peaks changes significantly from 3.4 at $P = 0$ to about 1.2 at $P = 3$ GPa and $T = 10$ K. These observations correspond to the significant decrease in the values of the ordered Mn magnetic moments and their reorientation in the *ab* plane. The angle φ between the Mn magnetic moments and hexagonal $\boldsymbol{a}$, $\boldsymbol{b}$ and $\boldsymbol{u} = -(\boldsymbol{a} + \boldsymbol{b})$ axes decreases continuously from 90° to 41° with increasing external pressure from 0 to 5 GPa (figure 3). This implies that the symmetry of the triangular AFM state of $YMnO_3$ changes from the pure Γ_1 ($\varphi = 90°$) to the mixed $\Gamma_1 + \Gamma_2$ irreducible representation (figure 3). In the latter model, arbitrary φ values are allowed between 90° and 0° with $\varphi = 0°$ corresponding to the pure Γ_2 representation. Assuming a linear pressure dependence of the φ value at $P > 5$ GPa as well, one can suggest the appearance of the pure Γ_2 magnetic phase at $P \sim 9$ GPa in $YMnO_3$ (figure 3).

In the pressure range 0–5 GPa, a significant reduction in the ordered Mn magnetic moment occurs from 3.27(5) to 1.52(9) μ_B at $T = 10$ K (table 1). Simultaneously, we also observed that, as we increase pressure from 0 to 5 GPa, there is a marked increase in the integrated intensity of the diffuse scattering peak located in the d-spacing range 4 Å $< d <$ 6 Å at 80 K, slightly above T_N (figure 1). These observations can be attributed to the enhancement of the spin fluctuations and considerable increase in the volume fraction of the spin-liquid state under high pressure. Since the halfwidth Δd_{dif} and the position of the diffuse peak d_{dif} depend weakly on pressure, the correlation length for the spin-liquid state is expected to remain nearly the same in the 0–5 GPa pressure range for $T = 80$ K. The estimated value of $\xi \approx 18$ Å obtained from the Selyakov–Scherrer formula $\xi \approx d_{dif}^2/\Delta d_{dif}$ is in good agreement with previous estimations for ambient pressure [9].

In $LuMnO_3$, a magnetic peak (101) at $d = 4.82$ Å and a magnetic contribution to the nuclear peak (102) at $d = 3.88$ Å at ambient pressure below $T_N \approx 90$ K appear. The refinements of the magnetic structure were initially made using magnetic structure models of Γ_2 and Γ_4 irreducible representations. Both models gave nearly the same fitting quality and values of ordered Mn magnetic moments. In order to discuss the high-pressure phenomena in $YMnO_3$ and $LuMnO_3$ in terms of equivalent models, we chose the Γ_2 representation model for further analysis of our high-pressure data. The value of the ordered Mn magnetic moment is

determined to be 2.48(5) μ_B at $T = 10$ K (table 1), which is comparable with that found in [3] and also considerably smaller than the expected value of 4.0 μ_B for Mn^{3+}.

As one can see in figure 2, the intensity of the magnetic peaks was observed to fall at high pressure. Subsequent data analysis has shown that the Γ_2 symmetry of the triangular AFM state remains unchanged, but the ordered Mn magnetic moment at the lowest temperature $T = 10$ K of our study decreases to 1.98(9) μ_B with increasing pressure up to 6 GPa (table 1). The reduction of the ordered magnetic moment in $LuMnO_3$ is much weaker than that in $YMnO_3$, indicating that a balance between the majority AFM ordered state and the minority spin-liquid state in $LuMnO_3$ is less affected by the application of high pressure. Therefore the change in the integrated intensity of the diffuse scattering peak located in the d-spacing range 4 Å $< d <$ 6 Å at $T \sim T_N$ was found to be small and comparable with the experimental accuracy for the pressure range studied (figure 2). We estimated the correlation length $\xi \approx$ 25–28 Å in the 0–6 GPa range.

In the hexagonal structure of $YMnO_3$ and $LuMnO_3$, the MnO_5 bi-pyramids consist of five Mn–O bonds: Mn–O1 and Mn–O2 oriented along the crystallographic c-axis while Mn–O3 and two pairs of Mn–O4 bonds lie within the *ab* plane. In our previous structural studies [16, 21] we found that, with increasing pressure, all four Mn–O bond lengths decrease continuously. As we noted before, the main exchange path is the Mn–O–Mn network on the *ab* plane. The O3 and O4 atoms are located close to the centres of triangles formed by Mn atoms (see figure 3) and the Mn–O3–Mn and Mn–O4–Mn have nearly 120° in-plane antiferromagnetic superexchange. Due to the difference in values of Mn–O3 and Mn–O4 bond lengths and Mn–O3–Mn and Mn–O4–Mn bond angles [16, 21], the strength of these interactions is slightly different from each other, and geometrical frustration effects are partially lifted, leading to the appearance of the various triangular ordered AFM arrangements in $RMnO_3$.

The difference between the dominant in-plane magnetic interactions is related to the distortion of the quasi-two-dimensional triangular network formed by Mn, O3, and O4 ions. In order to quantify the distortion, we have defined a parameter $s = (l_{Mn-O4} - l_{Mn-O3})/(l_{Mn-O4} + l_{Mn-O3})$, where l_{Mn-O3} and l_{Mn-O4} are Mn–O3 and Mn–O4 bond lengths. The Mn–O3–Mn and Mn–O4–Mn bond angles are close to 120°, and they change slightly with chemical substitution or external pressure [7–16, 21]. The modification of magnetic interactions due to changes in Mn–O–Mn bond angle is expected to be much smaller than those due to variations in the Mn–O3 and Mn–O4 bond lengths. For the ideal triangular lattice, the distortion parameter value is $s = 0$.

Figure 4 shows a dependence of the s value on the ionic radius of the R cation, calculated from high-resolution powder neutron diffraction and single-crystal x-ray diffraction data for $RMnO_3$ compounds [7, 12, 15, 21–25]. One can see a clear correlation between the distortion parameter s and the symmetry of the triangular AFM arrangement. For a relatively large value of $s \sim 0.025$ found for $YMnO_3$, the triangular AFM state of the Γ_1 symmetry is stable at ambient pressure, while for $ErMnO_3$, $YbMnO_3$ and $LuMnO_3$ with a much smaller $s \sim 0.001$–0.008 the Γ_2 (or Γ_4) symmetry of the triangular AFM state is realized instead. Interestingly enough, $HoMnO_3$ has the $s = 0.023$ value close to the boundary between Γ_1 and Γ_2 states, which we think is the main reason why it shows a spin-reorientation phase transition from the ground state Γ_1 to the intermediate state Γ_2 at $T_R = 45$ K [12]. In addition, it was found that an increase in Er content of $Y_{1-x}Er_xMnO_3$ leads to the decrease in ionic radius r and the gradual evolution of the magnetic state from Γ_1 to Γ_2 symmetry via the mixed $\Gamma_1 + \Gamma_2$ representation [25]. One may calculate from these data [25] that such a modification of the magnetic structure is accompanied by a decrease in the distortion parameter s value, in agreement with a derived generalized magnetic phase diagram (see figure 4).

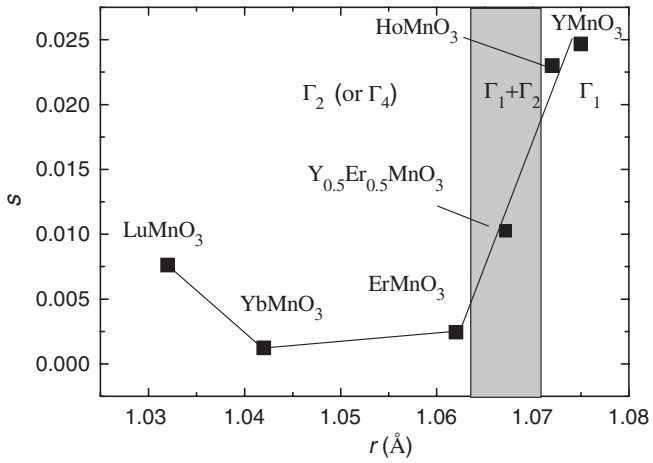

Figure 4. Generalized magnetic phase diagram of $RMnO_3$ hexagonal manganites in terms of the distortion parameter of the triangular network formed by Mn and O ions.

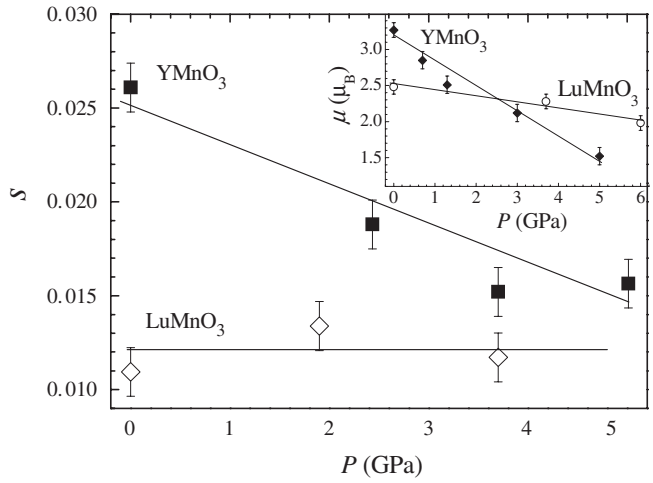

Figure 5. Pressure dependence of the distortion parameter of triangular network formed by Mn and O ions (at 295 K) and the ordered Mn magnetic moment (at 10 K) in $YMnO_3$ and $LuMnO_3$.

In $YMnO_3$, the s value decreases from 0.025 to 0.016 with increasing pressure up to 5 GPa (calculated from data [16]), while it remains nearly constant in $LuMnO_3$ (figure 5). Such a rapid decrease in s in $YMnO_3$ correlates with a change of the triangular AFM state symmetry from Γ_1 to Γ_2 through the mixed $\Gamma_1 + \Gamma_2$ representation and is consistent with the generalized magnetic phase diagram (figure 4) as well as with a rapid decrease in the ordered Mn magnetic moment (see the inset of figure 5).

The observed weak pressure dependence of s in $LuMnO_3$ (figure 5, calculated from data [21]) is also in good agreement with a stability of the triangular AFM state symmetry of Γ_2 representation in terms of the magnetic phase diagram of figure 4. It may as well explain why we observe a considerably small decrease in the ordered Mn magnetic moment under high pressure (figure 5) with $\mathrm{d}M/\mathrm{d}P = -0.08\ \mu_B\ \mathrm{GPa}^{-1}$ for $LuMnO_3$ in comparison with a much larger value of $-0.35\ \mu_B\ \mathrm{GPa}^{-1}$ for $YMnO_3$. The decrease in s is expected to enhance

geometrical frustration effects due to symmetrization of the triangular lattice, leading to the decrease in ordered magnetic moment.

4. Conclusions

The results of our study show that the formation of the magnetic phase diagram of hexagonal manganites is determined by the balance of two non-equivalent in-plane superexchange magnetic interactions. The difference between these interactions' strengths can be related to the distortion parameter characterizing the difference between two non-equivalent Mn–O bonds of the quasi-two-dimensional triangular network formed by Mn and O ions. The AFM triangular ground state of the Γ_1 irreducible representation symmetry is realized in $RMnO_3$ compounds with a large distortion parameter ($YMnO_3$ and $HoMnO_3$), while Γ_2 (or Γ_4) symmetry of the AFM ground state is preferred in those with a small distortion parameter ($LuMnO_3$, $YbMnO_3$, $ErMnO_3$).

The magnetic phase diagram of $RMnO_3$ hexagonal manganites in terms of the distortion parameter s can explain all the experimental key features. The decrease in the distortion parameter (s) by the application of high pressure (or chemical substitution) leads to the spin-reorientation phenomena from Γ_1 to Γ_2 symmetry, as observed experimentally in the present work for $YMnO_3$ and also previously for $Y_{1-x}Er_xMnO_3$. On the other hand, $LuMnO_3$ displays a tiny change in the distortion parameter, and thus the AFM ground state of the Γ_2 symmetry remains stable in the pressure range studied.

In $YMnO_3$ under pressure, due to a considerable decrease in the distortion parameter the quasi-two-dimensional triangular network formed by Mn and O ions approaches the ideal triangular network, and consequently the enhancement of geometrical frustration effects and spin fluctuations occur. These lead to suppression of the AFM ordered phase in favour of the spin-liquid state at high pressure. In $LuMnO_3$ the distortion parameter is a weak function of pressure, and the enhancement of frustration effects and spin fluctuations is much less pronounced.

Acknowledgments

Work at Sungkyunkwan University was supported by the Korea Research Foundation (grant no. KRF-2005-015-C00153), the Center for Strongly Correlated Materials Research, and the Basic Atomic Energy Research Institute program. Work at FLNP JINR was supported by the Russian Foundation for Basic Research, grant 06-02-81018-Bel-a. We thank the ISIS Facility, UK, for providing us with beam time at the GEM diffractometer for some of our high-pressure measurements. We acknowledge very useful discussions with, and help from, P G Radaelli and M G Tucker during the experiments at GEM, ISIS.

References

[1] Gilleo M A 1957 *Acta Crystallogr.* **10** 161
[2] Yakel H L, Koehler W C, Bertaut E F and Forrat E F 1963 *Acta Crystallogr.* **16** 957
[3] Katsufuji T, Masaki M, Machida A, Moritomo M, Kato K, Nishibori E, Takata M, Sakata M, Ohoyama K, Kitazawa K and Takagi H 2002 *Phys. Rev.* B **66** 134434
[4] Bertaut E F, Mercier M and Pauthenet R 1963 *Phys. Lett.* **5** 27
[5] Sato T J, Lee S-H, Katsufuji T, Masaki M, Park S, Copley J R D and Takagi H 2003 *Phys. Rev.* B **68** 014432
[6] Greedan J E, Bieringer M, Britten J F, Giaquinta D M and zur Loye H-C 1995 *J. Solid State Chem.* **116** 118
[7] Munoz A, Alonso J A, Martinez-Lope M J, Casais M T, Martinez J L and Fernandez-Dias M T 2000 *Phys. Rev.* B **62** 9498

[8] Park J, Kong U, Pirogov A, Choi S I, Park J-G, Choi I N, Lee C and Jo W 2002 *Appl. Phys.* A **74** (Suppl.) S796
[9] Park J, Park J-G, Jeon G S, Choi H Y, Lee C, Jo W, Bewley R, McEwen K A and Perring T G 2003 *Phys. Rev.* B **68** 104426
[10] Koehler W C, Yakel H L, Wollan E O and Cable J W 1964 *Phys. Lett.* **9** 93
[11] Fiebig M, Fröhlich D, Kohn K, Leute St, Lottermoser Th, Pavlov V V and Pisarev R V 2000 *Phys. Rev. Lett.* **84** 5620
[12] Munoz A, Alonso J A, Martinez-Lope M J, Casais M T, Martinez J L and Fernandez-Dias M T 2001 *Chem. Mater.* **13** 1497
[13] Lonkai Th, Hohlwein D, Ihringer J and Prandl W 2002 *Appl. Phys.* A **74** (Suppl.) S843
[14] Vajk O P, Kenzelmann M, Lynn J W, Kim S B and Cheong S-W 2005 *Phys. Rev. Lett.* **94** 087601
[15] Park J, Kong U, Choi S I, Park J-G, Lee C and Jo W 2002 *Appl. Phys.* A **74** (Suppl.) S802
[16] Kozlenko D P, Kichanov S E, Lee S, Park J-G, Glazkov V P and Savenko B N 2005 *JETP Lett.* **82** 193
[17] Janoschek M, Roessli B, Keller L, Gvasaliya S N, Conder K and Pomjakushina E 2005 *J. Phys.: Condens. Matter* **17** L425
[18] Glazkov V P and Goncharenko I N 1991 *High Pressure Phys. Tech.* **1** 56 (in Russian)
[19] Zlokazov V B and Chernyshev V V 1992 *J. Appl. Crystallogr.* **25** 447
[20] Rodriguez-Carvajal J 1993 *Physica* B **192** 55
[21] Kozlenko D P, Kichanov S E, Lee S, Park J-G, Glazkov V P and Savenko B N 2006 *JETP Lett.* **83** 346
[22] Van Aken B B, Meetsma A and Palstra T T M 2001 *Acta Crystallogr.* E **57** i101
[23] Van Aken B B and Palstra T T M 2004 *Phys. Rev.* B **69** 134113
[24] Van Aken B B, Meetsma A and Palstra T T M 2001 *Acta Crystallogr.* E **57** i87
[25] Sekhar M C, Lee S, Choi G, Lee C and Park J-G 2005 *Phys. Rev.* B **72** 014402